AIAA JOURNAL
Vol. 35, No. 7, July 1997

Technical Notes

TECHNICAL NOTES are short manuscripts describing new developments or important results of a preliminary nature. These Notes cannot exceed 6 manuscript pages and 3 figures; a page of text may be substituted for a figure and vice versa. After informal review by the editors, they may be published within a few months of the date of receipt. Style requirements are the same as for regular contributions (see inside back cover).

Design and Testing of a Subsonic All-Moving Adaptive Flight Control Surface

R. M. Barrett,* R. S. Gross,* and F. T. Brozoski†
Auburn University, Auburn, Alabama 36849-5338

Nomenclature

A, B, D	= extensional, coupling, and bending stiffness matrices
C_L	= lift coefficient
E_3	= through thickness electric field
E_L, E_T	= longitudinal and transverse element stiffness
l	= length of Flexspar component
N, M	= applied forces and moments
T	= thickness ratio, t_s/t_a
t	= thickness
ΔT	= temperature change
ε_{ij}	= ijth laminate strain
κ_{ij}	= ijth laminate curvature
Λ_i	= ith direction actuator free strains
ϕ	= pitch angle

Subscripts

a	= actuator
b	= bond
s	= substrate

Introduction

IN the past several years, tremendous strides have been made in the areas of smart structures and active flight control. In 1989, the foundation of active flight control using piezoelectric active elements was laid with the first series of experiments in the area of active aerodynamic surface manipulation. Crawley et al.[1] successfully showed that piezoelectric elements could be used to induce twist deflections in bending-twist and extension-twist coupled aerodynamic plates. Their invention was soon followed by a host of experimenters who showed that piezoceramic elements could induce twist and camber changes in aerodynamic surfaces. Many of these investigations were centered on aeroelastic tailoring and suppression of vibration and flutter. Ehlers and Weisshaar[2] built upon these original investigations by adding the effects of aeroservoelasticity and sweep.

At about the same time, efforts to improve the twist actuation capabilities of piezoceramic elements led to the invention of directionally attached piezoelectric elements. These specialized actuators were attached so that the normally isotropic piezoceramic actuators would be artificially given highly orthotropic properties. If the actuators were oriented at off-axis angles, then structures such as wings, missile fins, and rotor blades could be directly manipulated in torsion.

Following these early discoveries, a new design for an active missile fin was conceived in 1991. Because it was virtually impossible to twist or warp low-aspect-ratio missile fins to generate large changes in C_L, the newly invented torque-plate missile fin used active elements to pitch the entire aerodynamic shell. Testing showed that the small fin could generate $\pm$4.5-deg static pitch changes at high actuation potentials. Although these deflections generated ΔC_L levels that were an order of magnitude greater than wing warping, other methods were tried to further increase the deflections by using shell positioning and full-span, full-chord piezoceramic elements.

Further investigations into the area of active aeroservoelasticity showed that it was a property that was not well suited for flight control surfaces because of the buffet and divergence tendencies. Accordingly, a considerable amount of work has been directed toward increasing active control surface pitch deflections without using any aeroservoelastic coupling.

Although pitch deflections up to $\pm$8 deg have been achieved using torque-plate approaches, a lighter, simpler approach is needed for very light aerial vehicles. Accordingly, a new actuator arrangement using a Flexspar configuration was conceived, and about 20 different configurations were tested.[3] This Note is centered on the introduction of this new actuator concept, presenting first-order modeling techniques and illustrating the performance through a comparison of theory and experiment.

Flexspar Design and Modeling

Two major groups of Flexspars have been developed: 1) tip-joint, which is useful for high deflection and low force, and 2) shell joint, which is high force, low deflection. The tip-joint Flexspar uses a bender element, which is connected at the root to a fixed structural member. The tip of the bender is fitted with an extender, which is joined to the tip of the control surface. The shell-joint Flexspar is normally fixed at one end to the main spar and the other end to the leading and/or trailing edge of the inside of the shell.

Tip-Joint Flexspar

This newly invented pitch control actuator has several advantages over older configurations such as the torque-plate designs. Because it is built with only one actuator element, instead of a multitude of directionally attached components, it is much simpler and easier to build. Also, the design incorporates a motion amplification member, which increases pitch deflections by up to 50% over the torque-plate designs. Figure 1 shows the general arrangement of the tip-joint Flexspar design along with the active bender element and the end extender.

Shell-Joint Flexspar

Like the tip-joint Flexspar configuration, the shell-joint design is centered around simplicity. However, this design generally results in much higher equivalent torsional stiffnesses and better frequency response. Figure 2 shows the general arrangement of the shell-joint Flexspar.

Because the shell-joint design uses elements that need little or no increase in shell thickness, this design is amenable to transonic and supersonic surface design. The high pitch stiffness also gives the structure a higher bandwidth than the tip-joint configuration.

Received Jan. 12, 1996; revision received Feb. 6, 1997; accepted for publication March 26, 1997.

*Assistant Professor, Aerospace Engineering Department. Member AIAA.

†Graduate Research Assistant, Aerospace Engineering Department. Member AIAA.

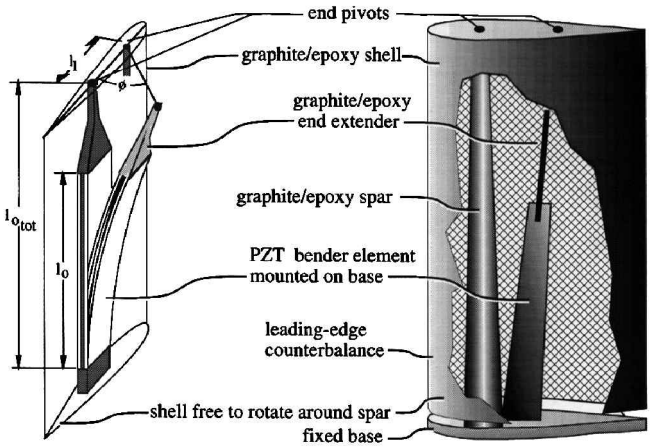

Fig. 1 Tip-joint Flexspar arrangement.

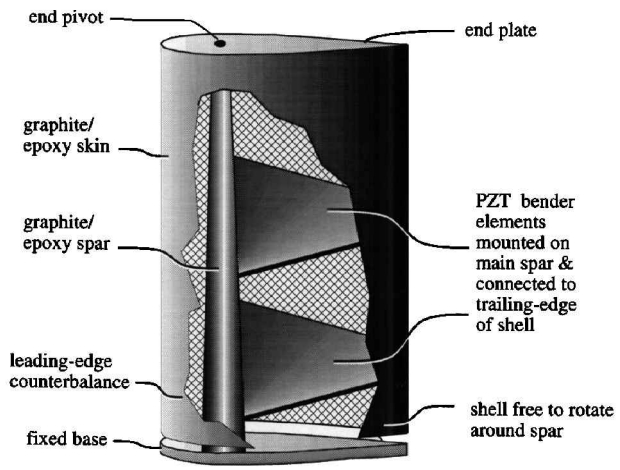

Fig. 2 Shell-joint Flexspar arrangement.

Flexspar Modeling

Using the techniques outlined in Ref. 4, the properties of the active elements may be easily characterized through laminated plate theory, assuming that the midplane strains are generated by external ex, actuator a, and thermally induced t moments and forces as follows:

$$\begin{Bmatrix} N \\ M \end{Bmatrix}_{\text{ex}} + \begin{Bmatrix} N \\ M \end{Bmatrix}_a + \begin{Bmatrix} N \\ M \end{Bmatrix}_t = \begin{bmatrix} A & B \\ B & D \end{bmatrix}_l + \begin{Bmatrix} \varepsilon \\ \kappa \end{Bmatrix}_l \tag{1}$$

If Eq. (1) is broken down for the thermally induced strains in a three-layer symmetric laminate of isotropic elements (as are the Flexspar actuators), then the laminate strain induced by an elevated temperature cure may be determined. (This is important for lending resistance to depoling.) Thus,

$$\varepsilon = \frac{(E_a A_a \bar{\alpha}_a + E_s A_s \bar{\alpha}_s)\Delta T}{(E_a A_a + E_s A_s)} = \frac{(\bar{\alpha}_a + \psi \bar{\alpha}_s)\Delta T}{(1+\psi)} \tag{2}$$

Tip-Joint Flexspar

The bending actuator for both kinds of Flexspars may be modeled by laminated plate theory. If an isotropic substrate is used and the stiffness of the bond is assumed to be negligible, then the bending curvature follows:

$$\kappa_{11} = \frac{E_a(t_s t_a + 2t_b t_a + t_a^2)\Lambda}{(E_s t_s^3/12) + E_a\left\{\left[(t_s + 2t_b)^2 t_a/2\right] + (t_s + 2t_b)t_a^2 + \frac{2}{3}t_a^3\right\}} \tag{3}$$

Employing the bending curvature of the actuator element, the amplified pitch deflection ϕ may be solved as a function of geometry. With the arrangement of Fig. 1, and solving for the kinematics of the system assuming $l_{0_{tot}}$ is relatively invariant due to the end pivot sliding through the bearing hole, the static, unloaded pitch angle ϕ may be determined as a function of bimorph curvature κ:

$$\phi = 2\sin^{-1}\left\{\frac{1-\cos(\kappa l_0)}{2l_1\kappa} + \left[\frac{l_{0_{tot}}}{2l_1} - \frac{\sin(\kappa l_0)}{2l_1\kappa}\right]\sin(\kappa l_0)\right\} \tag{4}$$

Shell-Joint Flexspar

Using the bending curvature estimation of Eq. (3) and assuming an element arranged as in Fig. 2, the pitch angle of the shell may be solved. Borrowing dimensional notation from Fig. 1 yields an expression for the pitch angle of the shell-joint Flexspar as a function of bender curvature:

$$\phi = \tan^{-1}\left\{\frac{1-\cos(\kappa l_0)}{l_{0_{tot}}\kappa} + \left[1 - \frac{\sin(\kappa l_0)}{l_{0_{tot}}\kappa}\right]\sin(\kappa l_0)\right\} \tag{5}$$

From Eq. (5) it can be seen that the shell-joint pitch angle will be considerably smaller than the tip-joint Flexspar configuration pitch angle for most control surface geometries. The frequency response, however, will be significantly improved over the tip-joint design.

Flexspar Stabilator Construction

Precompressed piezoceramic (PZT) sheets were incorporated into the Flexspar actuator. The tip-joint Flexspar design employed a pair of 5-mil-thick PZT-5H piezoceramic sheets, which were bonded to a 2-mil brass substrate. The bender actuators measured 2.5 in. long by 0.4 in. wide at the root by 0.3 in. at the tip. The elements of the actuator were joined by Scotchweld® epoxy tape and Masterbond® conducting epoxy in a 350¡F cure under approximately 8 psi of pressure. Following the cure, the element was removed from a pair of plate jigs and deflashed. Electrodes were attached to the substrate and the outer surfaces of the PZT sheets. After addition of the root and tip mounts, the actuator element was attached to the main spar at the base. A 2-in.-long graphite end extender was added to the element, which was joined to the tip of the Flexspar rotational member.

The structural members of the shell were constructed from a style #120 fiberglass leading-edge cuff, which was cocured with a graphite trailing edge. The tip of the element was also reinforced with fiberglass. The entire prototype actuator was covered by Micafilm® aerodynamic skin material (as shown in Fig. 3) and weighed only 0.39 oz (11 g).

Control Surface Testing

Several bench and wind-tunnel tests were conducted on the Flexspar specimen to determine actuation range and frequency response. The actuation range was determined by reflecting a laser beam off a mirror, which was mounted on the aerodynamic shell. The testing was conducted at 1 Hz with a sinusoidal signal input. After bench testing, wind-tunnel tests were conducted on the surface at 30 ft/s in the model-scale wind tunnel at Auburn University.

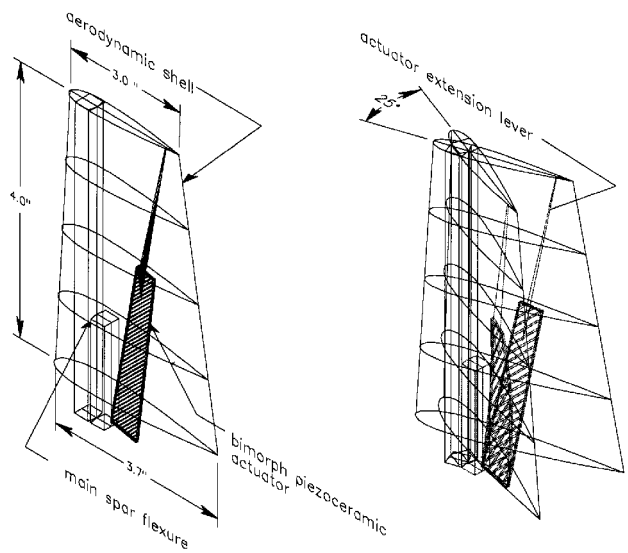

Fig. 3 Flexspar fin structure and geometry.

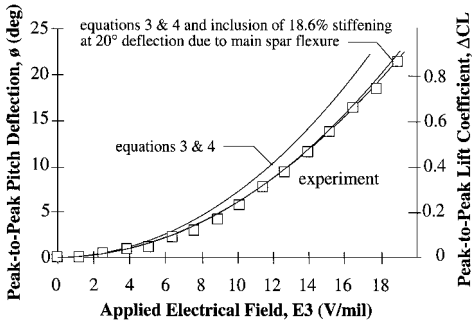

Fig. 4 Static pitch deflection with applied field.

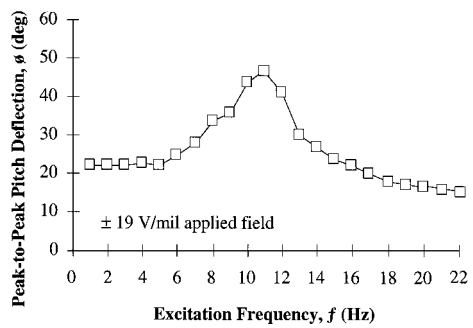

Fig. 5 Tip-joint Flexspar dynamic pitch deflection characteristics at ±19 V/mil.

Because of the mass balancing and collocation of the hinge line and aerodynamic center aeroelastic coupling and flutter were not detected. Figure 4 shows the static bench and wind-tunnel results.

From Fig. 4, it is clear that if the added stiffness of the main spar is included, then the error between theory and experiment drops to under 2%.

Following static testing, dynamic tests were conducted to determine the frequency response of the actuator. Figure 4 shows a natural frequency of approximately 11 Hz, and the break frequency of 23 maximum power consumption recorded during these tests was 40 mW.

The data of Figs. 4 and 5 clearly show that the tip-joint Flexspar generates very high deflections for given actuation potentials. The blunted peak at the natural frequency of approximately 11 Hz is caused by the shell bumping against the stops, which were set to approximately ±22 deg. From Fig. 4, the lift-curve slope may be resolved to approximately 0.039/deg. The low value of lift curve slope is primarily due to a significant amount of aerodynamic relieving that occurred at the base of the mount.

Conclusions

This study has shown that laminated plate theory and kinematics can successfully predict the deflections generated by piezoceramic Flexspar flight control surface actuators. Experimental model testing showed that pitch deflections up to ±11 deg may be achieved with Flexspar control surfaces measuring 4 in. in span with a 3.33-in. mean geometric chord. Dynamic testing demonstrated an 11-Hz natural frequency and a 23-Hz break frequency with 40 mW of power consumed at the most extreme actuation condition.

Acknowledgments

The authors would like to acknowledge the Auburn University School of Engineering and Aerospace Engineering Department for supporting this research, along with Brian Chin and the Auburn University Materials Engineering Program. The authors would also like to thank Clifton Minter, Steven Williams, and Steven Rose for helping with the construction of the Flexspar fins.

References

[1]Crawley, E. F., Lazarus, K. B., and Warkentin, D. J., "Embedded Actuation and Processing in Intelligent Materials," 2nd International Workshop on Composite Materials and Structures (Troy, NY), Army Research Office, Research Triangle Park, NC, Sept. 1982.

[2]Ehlers, S. M., and Weisshaar, T. A., "Static Aeroelastic Behavior of an Adaptive Laminated Piezoelectric Composite Wing," *AIAA Journal*, Vol. 28, No. 4, 1990, pp. 1611–1623.

[3]Barrett, R., Gross, R. S., and Brozoski, F., "Missile Flight Control Using Active Flexspar Actuators," *Proceedings of the Society of Photo-Optical Instrumentation Engineers 1995 Smart Structures and Materials Conference* (San Diego, CA), Vol. 2443, Society of Photo-Optical Instrumentation Engineers, Bellingham, WA, 1995, pp. 52–61.

[4]Jones, R. M., "Micromechanical Behavior of a Lamina," *Mechanics of Composite Materials*, Hemisphere, New York, 1975, pp. 147–237.

R. K. Kapania
Associate Editor

Interface Wavelength Between Confined Supersonic Two-Dimensional Jets and Subsonic Streams

Lawrence J. De Chant,* Jerald A. Caton,† and Malcolm J. Andrews‡
Texas A&M University, College Station, Texas 77843

Nomenclature

A = cross-sectional area
g = gravitational constant
H_s = splitter plate height
M = Mach number
P = total pressure
p = static pressure
T = temperature
U = free/mainstream velocity
u = streamwise velocity
v = cross-stream velocity
x = streamwise coordinate
β = $(M^2 - 1)^{1/2}$
γ = ratio of specific heats
ε = small perturbation term, $1 - U_1/U_{1s}$
ξ = dimensionless interface amplitude, $(\beta_{1s})^2[1 - U_1/U_{1s}]$
ρ = density
ϕ = small disturbance velocity potential

Subscripts

c = critical
eff = effective state
s = streamline value
0 = stagnation or reservoir condition
1, 2 = primary and secondary streams

Introduction

A MODEL for the freejet interface wavelength of an inviscid, supersonic and subsonic stream is described. The model, which is a confined flow extension to a previous methodology, involves modifying the lowest-order perturbation quantities to honor internal flow conservation and to provide the first critical location of the slipline. We show reasonable agreement between the model and analog measurements for the critical wavelength.

Received Dec. 20, 1996; revision received March 27, 1997; accepted for publication April 10, 1997.

*Graduate Research Assistant, Department of Mechanical Engineering, MS 3123.

†Professor, Department Head, Department of Mechanical Engineering, MS 3123. Member AIAA.

‡Assistant Professor, Department of Mechanical Engineering, MS 3123. Member AIAA.